

Quasinormal modes and shadows of a new family of Ayón-Beato-García black holes

Xin-Chang Cai* and Yan-Gang Miao†

School of Physics, Nankai University, Tianjin 300071, China

Abstract

We obtain a type of Ayón-Beato-García (ABG) related black hole solutions with five parameters: the mass m , the charge q , and three dimensionless parameters α , β and γ associated with nonlinear electrodynamics. We find that this type of black holes is regular under the conditions: $\alpha\gamma \geq 6$, $\beta\gamma \geq 8$, and $\gamma > 0$. Here we focus on the saturated case: $\alpha = 6/\gamma$ and $\beta = 8/\gamma$, such that only three parameters m , q and γ remain, which leads to a new family of ABG black holes. For such a family of black holes, we investigate the influence of the charge q and the parameter γ on the horizon radius and the Hawking temperature. In addition, we calculate the quasinormal mode frequencies of massless scalar field perturbations by using the sixth-order WKB approximation method and the unstable circular null geodesic method in the eikonal limit. On the one hand, our results show that the increase of the charge q makes the scalar waves decay faster at first and then slowly except for the case of $\gamma = 2$. On the other hand, they show that the increase of the parameter γ makes the scalar waves decay at first sharply and then slowly. In particular, $\gamma = 1$ can be regarded as the critical value for the transition from an unstable configuration to a stable one. Finally, we compute the shadow radius for the new family of ABG black holes and use the shadow data of the $M87^*$ black hole detected by the Event Horizon Telescope to provide an upper limit on the charge q of the new black holes. We find that the increase of the charge q makes the shadow radius decrease monotonically, while the increase of the parameter γ makes the shadow radius increase at first rapidly and then almost remain unchanged, especially the parameter γ has a significant impact on the shadow radius when it is less than one. Moreover, using the shadow data of the $M87^*$ black hole, we find that the upper limit of the charge q increases rapidly at first and then slowly but does not exceed the mass of the $M87^*$ black hole at last when the parameter γ is increasing and going to infinity, and that the data restrict the frequency range of the fundamental mode with $l = 1$ to $1.4 \times 10^{-6} \text{Hz} \sim 1.9 \times 10^{-6} \text{Hz}$.

*E-mail address: caixc@mail.nankai.edu.cn

†Corresponding author. E-mail address: miaoyg@nankai.edu.cn

1 Introduction

It is well known that the black hole solutions of Einstein's field equations have a spacetime singularity which cannot be eliminated by coordinate transformations. In fact, the singularity theorem proved by Penrose and Hawking [1, 2] shows that the existence of singularities in general relativity is inevitable under some reasonable physical conditions. Since the spacetime singularity inside a black hole can lead to the failure of all physical laws, Penrose proposed [3, 4] the famous cosmic supervision hypothesis in 1969: The spacetime singularity is always hidden by the event horizon of black holes. However, it is widely believed [5] that spacetime singularities are unphysical objects that should not exist in nature due to limitations of classical theories of gravity, and that these singularities can be avoided especially when quantum effects are taken into account. Based on this idea, Bardeen proposed [6] the first static spherically symmetric regular black hole solution with an unknown physical source. Later, Ayón-Beato and García realized [7] that the physical source of regular black holes may be a nonlinear electromagnetic field, and under the framework of general relativity, they successfully obtained [7–10] a series of regular black hole solutions by coupling an appropriate field of nonlinear electrodynamics to Einstein's field equations. In this way, many regular black hole solutions have been obtained [5, 11–13] so far.

Inspired by Ref. [5], we notice that the metric function $f(r)$ of regular black hole solutions with magnetic charges or electric charges can contain a term like $r^a/(r^b + q^b)^{a/b}$, where a and b are two dimensionless parameters associated with nonlinear electrodynamics, and then obtain a type of ABG related black hole solutions. Within this framework of black hole solutions, the ABG black hole solution [7] and its generalization [10] become the special cases of this type of ABG related black hole solutions. Our fulfilment may be a further improvement of the ABG black hole and its generalized solutions.

Recently, the gravitational waves from the merger of two black holes detected by LIGO and Virgo collaborations [14, 15] and the first black hole image detected by the Event Horizon Telescope (EHT) collaboration [16, 17] have greatly stimulated the enthusiasm for black hole physics. The two achievements represent the significance of black hole perturbations and black hole shadows, respectively. So far, the quasinormal modes and the shadows of a large number of black hole models have been widely and deeply analyzed, for instance, see Refs. [18–51]. We hope the construction of a type of ABG related black hole solutions will expand the family of ABG black holes and promote the related studies in quasinormal modes and shadows.

The paper is organized as follows. In Sec. 2, we construct a type of ABG related black hole solutions. Then, we investigate in Sec. 3 the characteristics of its saturated form — a new family of ABG black holes. We compute the quasinormal mode frequencies of massless scalar field perturbations in Sec. 4 and the shadows in Sec. 5 for this new family of black holes. Finally, we make a simple summary in Sec. 6. We use the units $c = G = k_B = \hbar = 1$ and the sign convention $(-, +, +, +)$ throughout this paper.

2 Construction of a type of ABG related black holes

The action of Einstein's gravity coupled to a nonlinear electrodynamic field takes [7–10] the form,

$$S = \int d^4x \sqrt{-g} \left[\frac{1}{16\pi} R - \frac{1}{4\pi} L(P) \right]. \quad (1)$$

Here R is the scalar curvature, $L(P) = 2PH_P - H(P)$ is a function of the invariant $P \equiv \frac{1}{4}P_{\mu\nu}P^{\mu\nu}$, and the antisymmetric tensor $P_{\mu\nu} \equiv F_{\mu\nu}/H_P$, where $H_P \equiv dH(P)/dP$, $H(P)$ is the structure function of the nonlinear electrodynamic theory corresponding to the nonlinear electromagnetic tensor $F_{\mu\nu} \equiv \partial_\mu A_\nu - \partial_\nu A_\mu$ with the electromagnetic potential A_μ .

Varying Eq. (1) with respect to the metric $g_{\mu\nu}$ and the electromagnetic potential A_μ , respectively, one can derive [7–10] the Einstein field equations coupled with nonlinear electrodynamics as follows,

$$G_\mu^\nu = 2[H_P P_{\mu\lambda} P^{\nu\lambda} - \delta_\mu^\nu (2PH_P - H(P))], \quad (2)$$

$$\nabla_\mu P^{\nu\mu} = 0. \quad (3)$$

A static spherically symmetric black hole can be described by the line element,

$$ds^2 = -f(r)dt^2 + \frac{dr^2}{f(r)} + r^2(d\theta^2 + \sin^2\theta d\phi^2), \quad (4)$$

where $f(r)$ is the metric function. By assuming $P_{\mu\nu} = 2\delta_{[\mu}^t \delta_{\nu]}^r D(r)$, where $D(r)$ is a function of r , and combining the line element Eq. (4) with Eq. (3), one can get [7, 8, 10]

$$P_{\mu\nu} = 2\delta_{[\mu}^t \delta_{\nu]}^r \frac{q}{r^2} \implies P = -\frac{D^2}{2} = -\frac{q^2}{2r^4}, \quad (5)$$

where q is integral constant that acts as electric charge. Note that q specifically refers to as $|q|$ since parameter γ appeared in the formula below may take an odd number. We choose such a structure function,

$$H(P) = \frac{P \left[1 - \left(\frac{\beta\gamma}{2} - 1 \right) (-2Pq^2)^{\gamma/4} \right]}{\left[(-2Pq^2)^{\gamma/4} + 1 \right]^{\frac{\beta}{2}+1}} - \frac{\alpha\gamma m (-2Pq^2)^{\frac{\gamma+3}{4}}}{2q^3 \left[(-2Pq^2)^{\gamma/4} + 1 \right]^{\frac{\alpha}{2}+1}}, \quad (6)$$

where α , β , and γ are three dimensionless parameters and m is a parameter related to mass. If $\gamma > 1$, for the weak field limit, $P \ll 1$, we have $H \approx P$, which means that the nonlinear electrodynamics returns to Maxwell's theory; if $0 < \gamma < 1$, we have $H \approx -\alpha\gamma m (-2Pq^2)^{(\gamma+3)/4} / (2q^3)$ under the weak field limit, which implies that the nonlinear electrodynamics does not return to Maxwell's theory. Therefore, $\gamma = 1$ is an important critical value of this nonlinear theory.

By substituting Eqs. (4)-(6) into Eq. (2), we obtain the metric function,

$$f(r) = 1 - \frac{2mr^{\frac{\alpha\gamma}{2}-1}}{(q^\gamma + r^\gamma)^{\alpha/2}} + \frac{q^2 r^{\frac{\beta\gamma}{2}-2}}{(q^\gamma + r^\gamma)^{\beta/2}}, \quad (7)$$

which is a type of Ayón-Beato-García (ABG) related black hole solutions. It is easy to see that this type of solutions returns to the ABG black hole solution [7] when $\alpha = 3$, $\beta = 4$, and $\gamma = 2$, and to the generalized ABG black hole solution [10] when $\gamma = 2$.

Combining Eq. (4) and Eq. (7), we can calculate the Ricci scalar of this type of ABG related black holes,

$$R = \frac{\alpha\gamma m q^\gamma r^{\frac{\alpha\gamma}{2}-3} [(\alpha\gamma+2)q^\gamma - 2(\gamma-1)r^\gamma]}{2(r^\gamma + q^\gamma)^{\frac{\alpha}{2}+2}} - \frac{\beta\gamma q^{\gamma+2} r^{\frac{\beta\gamma}{2}-4} [(\beta\gamma-2)q^\gamma - 2(\gamma+1)r^\gamma]}{4(r^\gamma + q^\gamma)^{\frac{\beta}{2}+2}}. \quad (8)$$

Similarly, we can also obtain the curvature invariants, $R_{\mu\nu}R^{\mu\nu}$ and $R_{\mu\nu\rho\sigma}R^{\mu\nu\rho\sigma}$. We conclude that the three invariants converge at $r = 0$ under the conditions: $\alpha\gamma \geq 6$, $\beta\gamma \geq 8$, and $\gamma > 0$, which means that the type of ABG related black holes is regular.

If the above conditions are saturated, i.e. $\alpha = \frac{6}{\gamma}$ and $\beta = \frac{8}{\gamma}$, we give a new family of ABG black holes with the metric function,

$$f(r) = 1 - \frac{2mr^2}{(r^\gamma + q^\gamma)^{3/\gamma}} + \frac{q^2 r^2}{(r^\gamma + q^\gamma)^{4/\gamma}}, \quad (9)$$

which contains three parameters, m , q , and γ , and satisfies the weak energy condition, i.e. $H(P) < 0$ and $H_P > 0$. In addition, Eq. (9) returns to the metric function of the Reissner-Nordström black hole solution when $\gamma \rightarrow \infty$.

3 Characteristics of the new family of ABG black holes

By using Eq. (9) and the formula of Hawking temperature [53, 54], $T_H = \frac{1}{4\pi}f'(r_H)$, we can calculate the Hawking temperature for the new family of ABG black holes,

$$T_H = \frac{r_H^\gamma \left[1 - q^2 r_H^2 (r_H^\gamma + q^\gamma)^{-4/\gamma} \right] - 2q^\gamma}{4\pi r_H (r_H^\gamma + q^\gamma)}, \quad (10)$$

where r_H is the event horizon radius.

In Fig. 1, we plot the metric function $f(r)$, Eq. (9), with respect to r for different values of charge q when γ is given for different cases. We can see that this family of black holes may have none, or one, or two horizons as the charge q decreases, which is just like the behaviour of the ABG black hole and Reissner-Nordström black hole. We note that the smaller the parameter γ is, the smaller the charge q of the extreme black hole is, see the values of q corresponding to blue curves.

In Fig. 2, we plot the extreme event horizon radius r_{EH} with respect to the parameter γ . We can see that the increase of the parameter γ makes the extreme event horizon radius increase at first and then decrease, especially there exists a special value of parameter γ that maximizes the extreme event horizon radius, which is associated with the structure of the nonlinear electrodynamics, see the analysis of the structure function in section 2.

In Fig. 3, we plot the Hawking temperature T_H with respect to the event horizon radius r_H for different values of charge q when γ is given for different cases. We can see that the increase of the event horizon radius r_H makes the Hawking temperature T_H increase at first and then decrease, and the increase of the charge q makes the Hawking temperature decrease. This behaviour is just like that of the ABG black hole and Reissner-Nordström black hole. In addition, we can also see that the Hawking temperature increases more and more slowly with the increasing of parameter γ for a fixed q .

4 Quasinormal mode frequencies of massless scalar field perturbations for the new family of ABG black holes

In this section, we study the quasinormal modes of a neutral massless scalar field perturbation around one of the new ABG black holes. The propagation of the massless scalar field Φ in the curved spacetime

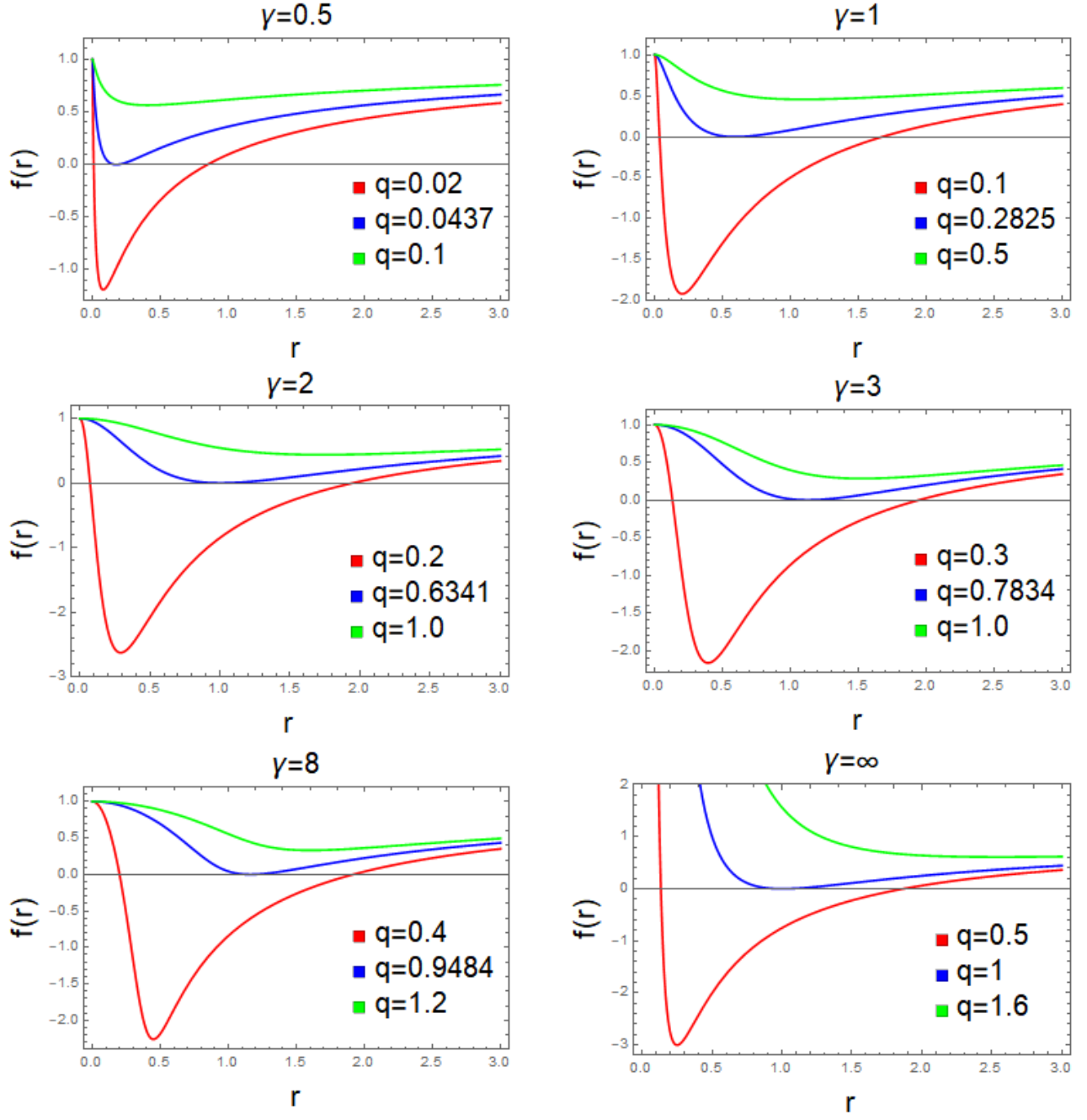


Fig. 1. Function $f(r)$ with respect to r for different values of charge q when parameter γ is given for different cases, where the case of $\gamma = 2$ corresponding to the ABG black hole and the case of $\gamma \rightarrow \infty$ to the Reissner-Nordström black hole are attached for comparison. Here we set $m = 1$.

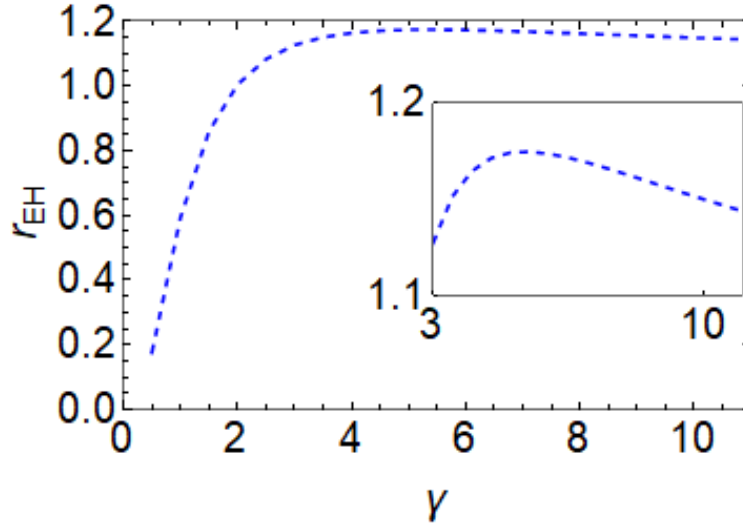


Fig. 2. The extreme event horizon radius r_{EH} with respect to the parameter γ . Here we set $m = 1$.

depicted by Eq. (9) is described by the Klein-Gordon equation,

$$\frac{1}{\sqrt{-g}} \partial_\mu (\sqrt{-g} g^{\mu\nu} \partial_\nu \Phi) = 0, \quad (11)$$

where g is the determinant of the metric tensor $g_{\mu\nu}$. By defining the tortoise coordinate $dr_* \equiv \frac{dr}{f(r)}$ and substituting $\Phi = e^{-i\omega t} Y_{lm}(\theta, \varphi) \frac{\Psi(r)}{r}$ together with Eqs. (4) and (9) into Eq. (11), we obtain

$$\frac{d^2 \Psi(r_*)}{dr_*^2} + [\omega^2 - V(r)] \Psi(r_*) = 0, \quad (12)$$

with the effective potential,

$$V(r) = \left[1 - \frac{2mr^2}{(q^\gamma + r^\gamma)^{3/\gamma}} + \frac{q^2 r^2}{(q^\gamma + r^\gamma)^{4/\gamma}} \right] \left\{ \frac{(l+1)l}{r^2} + \frac{2 \left[m(r^\gamma - 2q^\gamma)(q^\gamma + r^\gamma)^{1/\gamma} + q^2(q^\gamma - r^\gamma) \right]}{(q^\gamma + r^\gamma)^{\frac{\gamma+4}{\gamma}}} \right\}, \quad (13)$$

where ω is complex quasinormal mode frequency and l multipole number.

4.1 Quasinormal mode frequencies of massless scalar field perturbations by the sixth-order WKB approximation

We use the WKB approximation method to calculate numerically the quasinormal mode frequencies of massless scalar field perturbations for the new family of ABG black holes. This method has been developed [55–58] from the first order to the latest 13th order. We choose the sixth-order WKB approximation method for the sake of the computational efficiency and accuracy. Then, we draw the graphs of real parts and negative imaginary parts of quasinormal mode frequencies with respect to the charge q and the parameter γ , as shown in Fig. 4 and Fig. 5, respectively. We note that the charge q in Fig. 4 ends with the values corresponding to the extreme configurations as shown by the blue curves in Fig. 1.

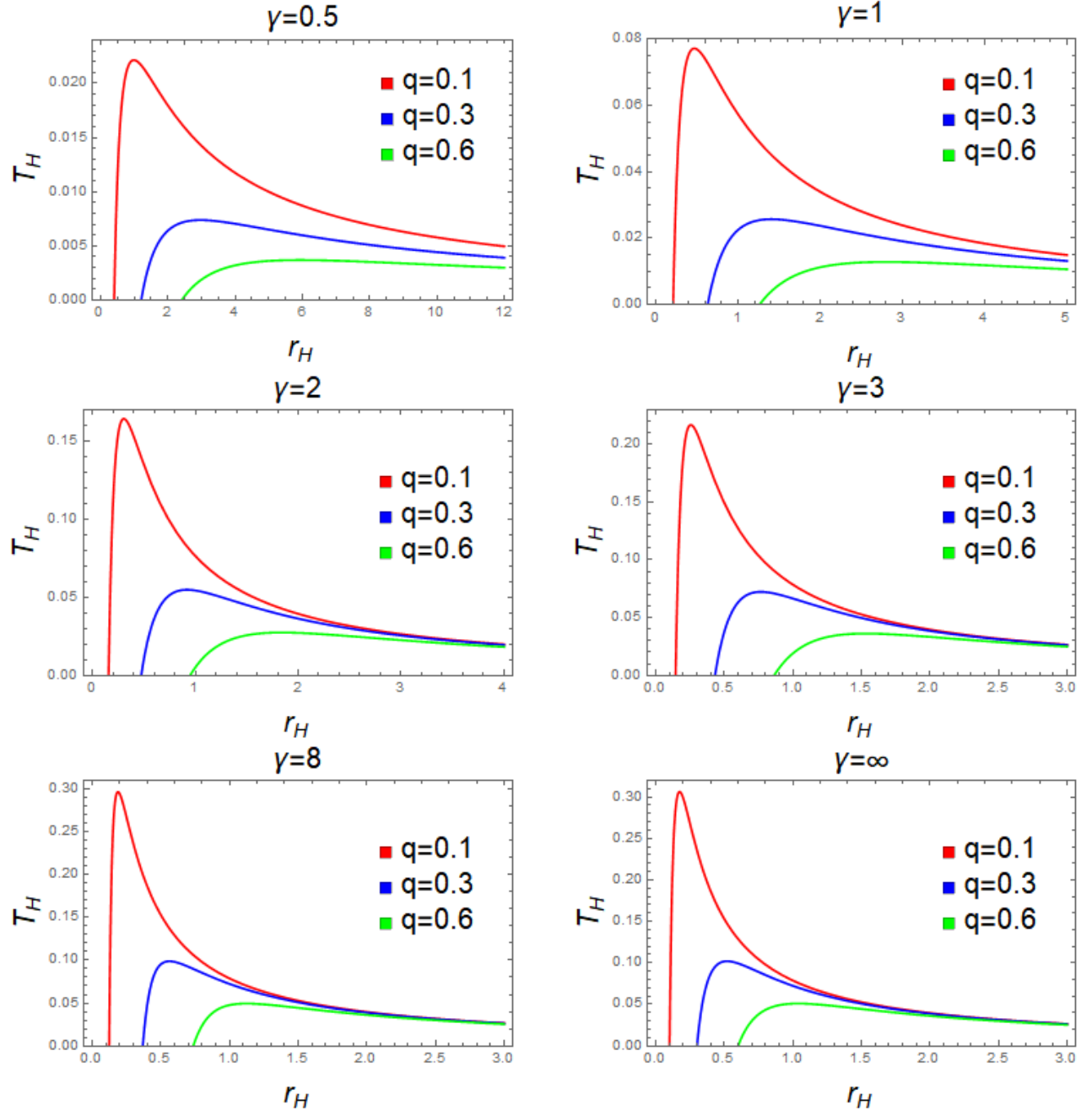
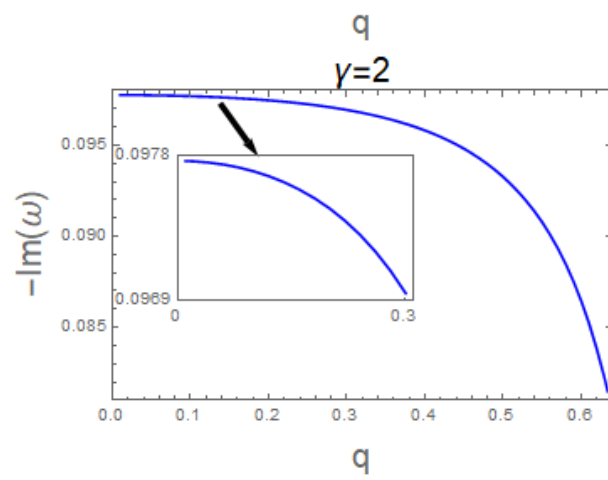
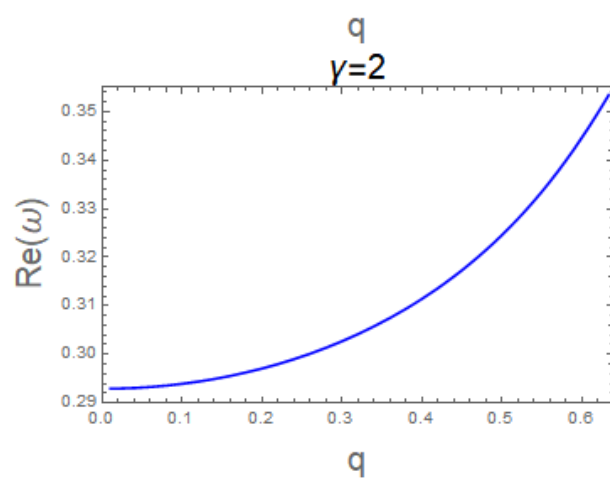
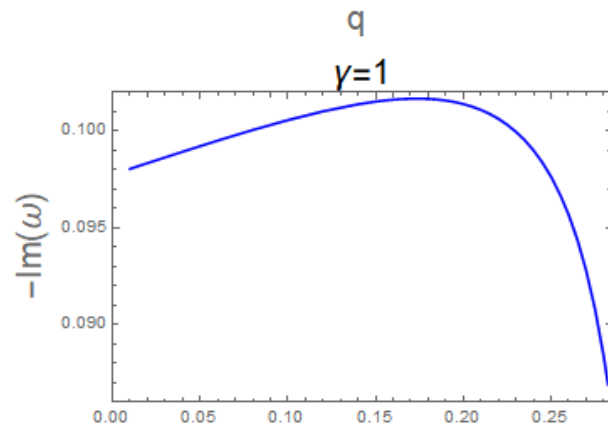
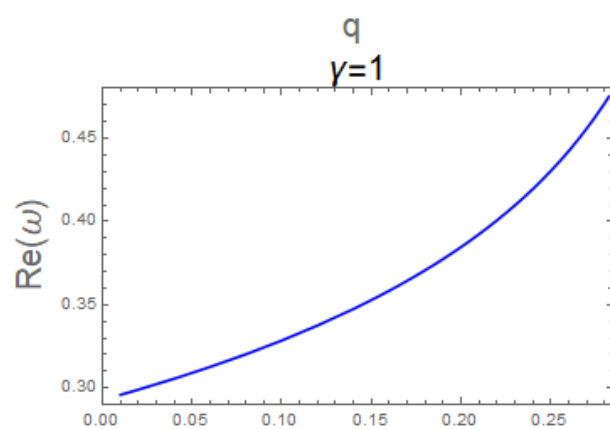
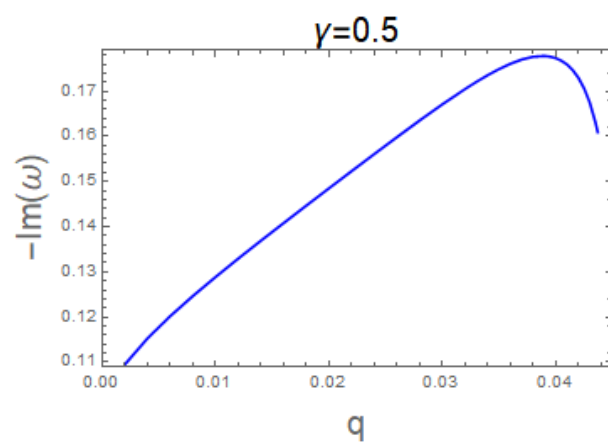
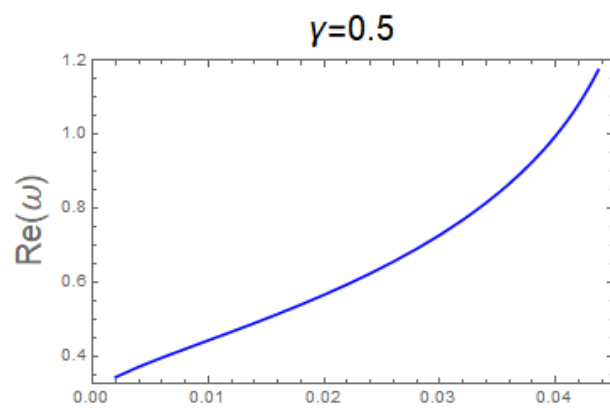


Fig. 3. The Hawking temperature T_H with respect to the event horizon radius r_H for different values of charge q when parameters γ is given for different cases, where the case of $\gamma = 2$ corresponding to the ABG black hole and the case of $\gamma \rightarrow \infty$ to the Reissner-Nordström black hole are attached for comparison.



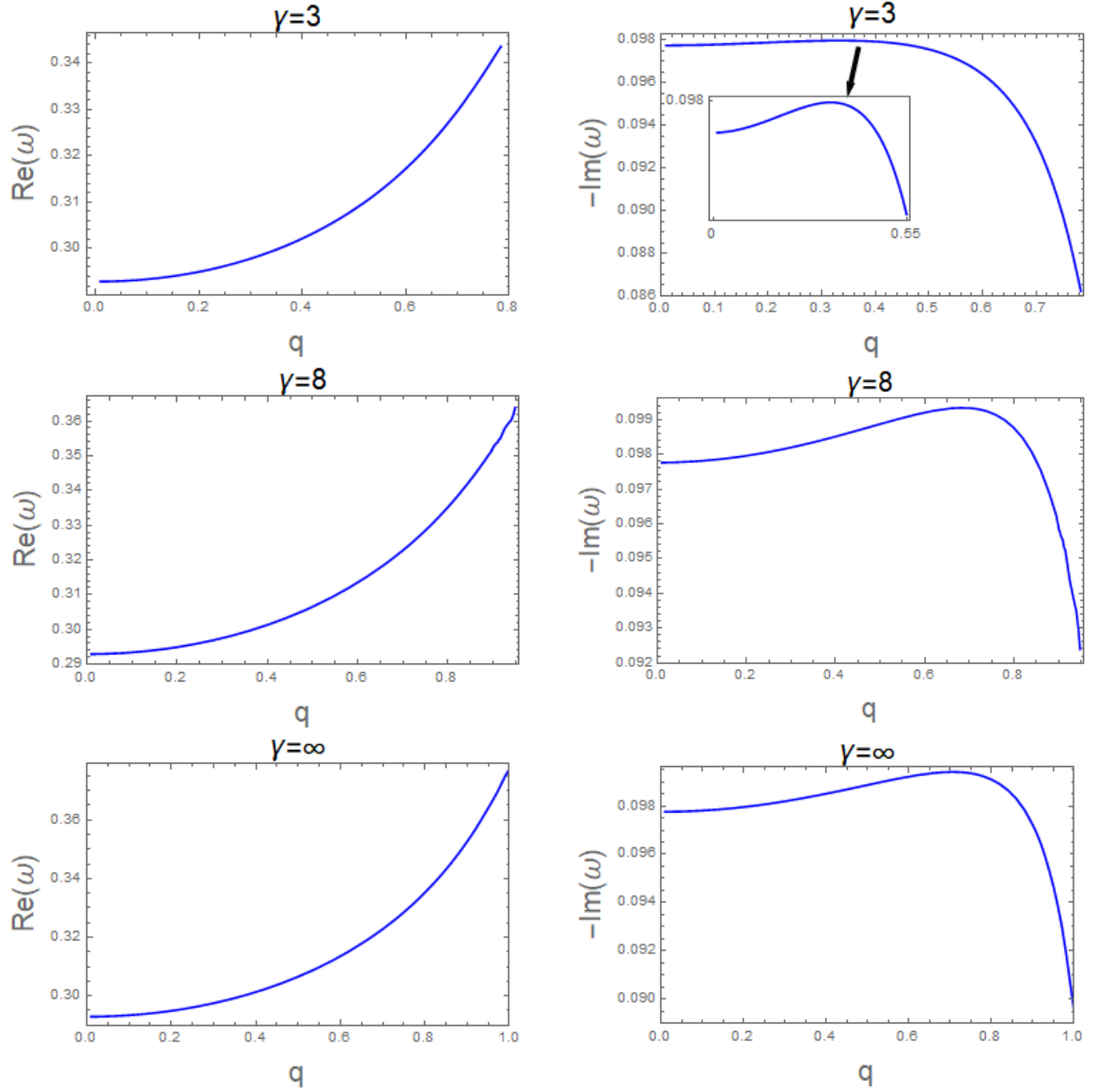


Fig. 4. The real parts and negative imaginary parts of quasinormal mode frequencies of massless scalar field perturbations with respect to the charge q when γ is given for different cases, where the case of $\gamma = 2$ corresponding to the ABG black hole and the case of $\gamma \rightarrow \infty$ to the Reissner-Nordström black hole are attached for comparison. Here we set $m = 1$, $l = 1$, and $n = 0$.

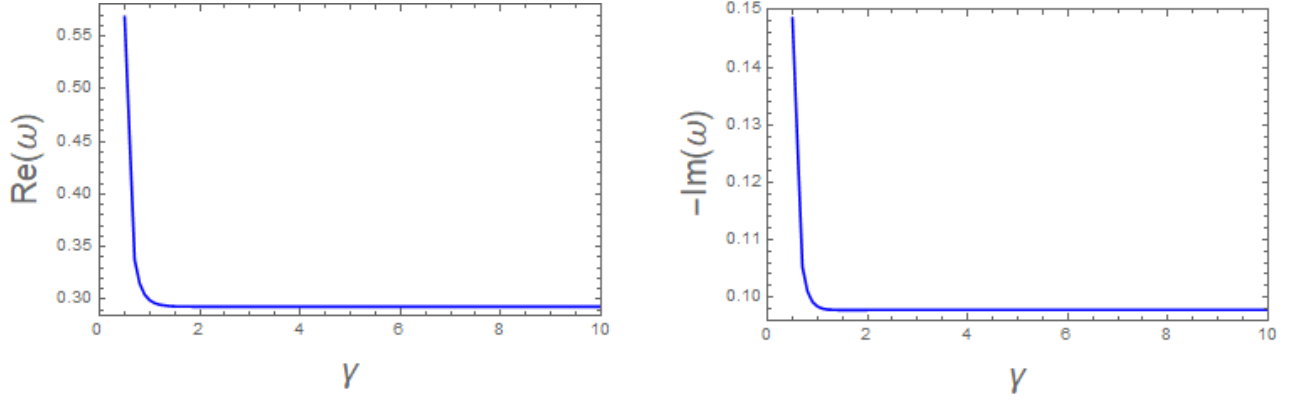


Fig. 5. The real parts and negative imaginary parts of quasinormal mode frequencies of massless scalar field perturbations with respect to the parameters γ . Here we set $m = 1$, $q = 0.02$, $l = 1$, and $n = 0$.

From Fig. 4 we can see that the behaviour of quasinormal modes of the new family of ABG black holes is similar to that of the Reissner-Nordström black hole as the charge q increases except for the case of $\gamma = 2$ — the ABG black hole. That is, the real parts increase monotonically, while the negative imaginary parts increase at first to the maximum and then decrease for the new family of ABG black holes, which means that the scalar wave decays fast at the beginning and then slowly as the charge q increases except for the ABG black hole.

From Fig. 5 we can see that both the real parts and negative imaginary parts decrease sharply and then almost remain unchanged as the parameter γ increases, which shows that the scalar wave decays quickly at first and then slowly. This phenomenon implies that the parameter γ has a significant impact on the quasinormal mode frequencies when $0 < \gamma < 1$. In particular, $\gamma = 1$ can be regarded as the critical value for the transition from an unstable to a stable configuration of new ABG black holes because $\gamma = 1$ is an important critical value of the nonlinear electrodynamics as mentioned in section 2.

4.2 Quasinormal mode frequencies in the eikonal limit calculated via the unstable circular null geodesics

The unstable circular null geodesic method was first proposed by Cardoso et al. [59] for calculation of the quasinormal mode frequencies of a static spherically symmetric black hole in the eikonal limit, $l \gg 1$. The effective potential Eq. (13) reduces to the following form in this limit,

$$V(r) = \left[1 - \frac{2mr^2}{(q^\gamma + r^\gamma)^{3/\gamma}} + \frac{q^2 r^2}{(q^\gamma + r^\gamma)^{4/\gamma}} \right] \frac{l^2}{r^2}, \quad (14)$$

and the corresponding quasinormal mode frequencies are determined [59–61] by

$$\omega_{l \gg 1} = l\Omega_c - i \left(n + \frac{1}{2} \right) |\lambda_L|, \quad (15)$$

with

$$\Omega_c = \frac{\sqrt{f(r_c)}}{r_c}, \quad \lambda_L = \sqrt{\frac{f(r_c)[2f(r_c) - r_c^2 f''(r_c)]}{2r_c^2}}, \quad (16)$$

where the angular velocity Ω_c and the Lyapunov exponent λ_L control the real parts and imaginary parts of the quasinormal mode frequencies ω , respectively. Moreover, the radius r_c of circular null geodesics is given by

$$2f(r_c) - r_c \left. \frac{df(r)}{dr} \right|_{r=r_c} = 0. \quad (17)$$

As discussed in the above subsection, we plot the graphs of the angular velocity Ω_c and the Lyapunov exponent λ_L with respect to the charge q and the parameter γ in Fig. 6 and Fig. 7, respectively. By comparing Fig. 4 with Fig. 6 and Fig. 5 with Fig. 7, we conclude that the two methods coincide with each other.

5 Shadows of the new family of ABG black holes

We investigate the shadow radius of the new family of ABG black holes. The shadow radius of a static spherically symmetric black hole observed by a static observer at infinity takes [51, 52, 62, 63] the form,

$$R_{\text{sh}} = \frac{1}{\Omega_c} = \frac{r_c}{\sqrt{f(r_c)}}. \quad (18)$$

In Fig. 8, we plot the shadow radius R_{sh} with respect to the charge q when γ is given for different cases. We can see that the shadow radius decreases monotonically as the charge q increases, which is inverse to the behaviour of the real parts as shown in Fig. 4 and Fig. 6.

In Fig. 9, we plot the shadow radius R_{sh} with respect to the parameter γ for a fixed charge, $q = 0.02$. We can see that the shadow radius increases rapidly at first and then almost remains unchanged as the parameter γ increases, which shows that the parameter γ has a significant impact on the shadow radius when it is less than one. This is inverse to the behaviour of the real parts as shown in Fig. 5 and Fig. 7.

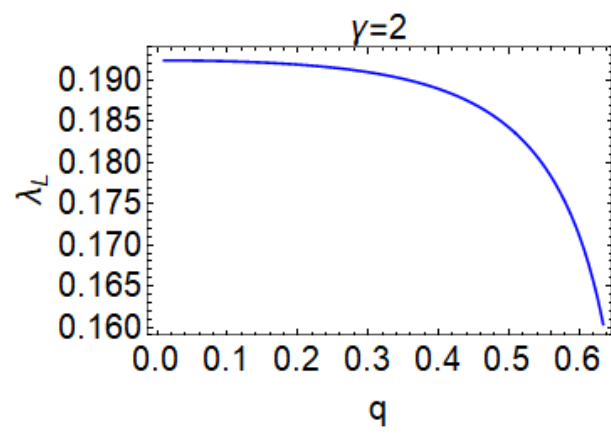
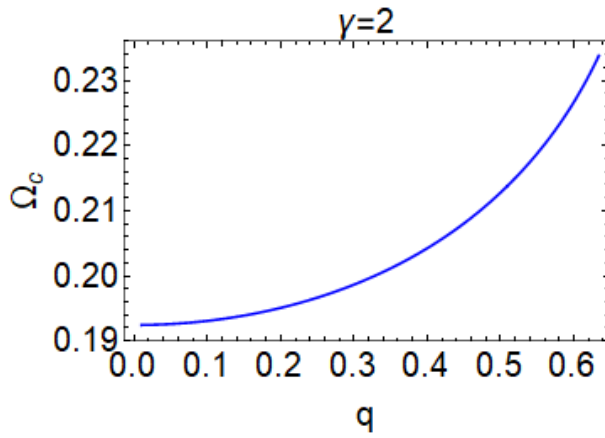
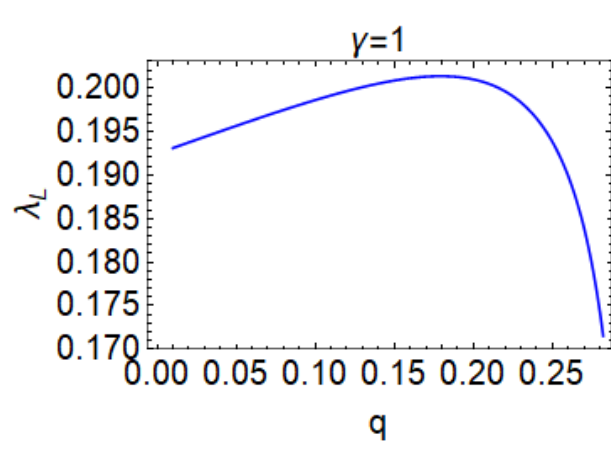
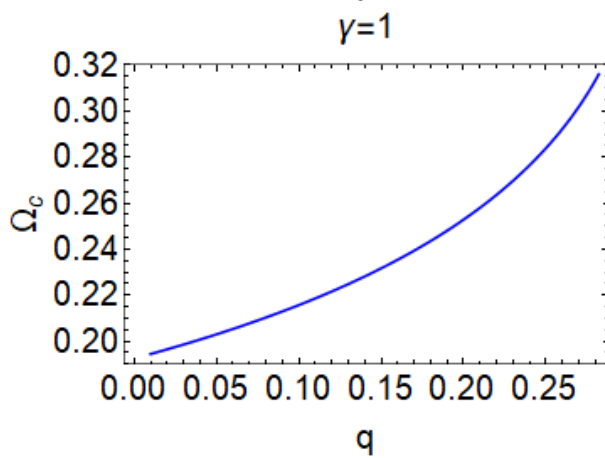
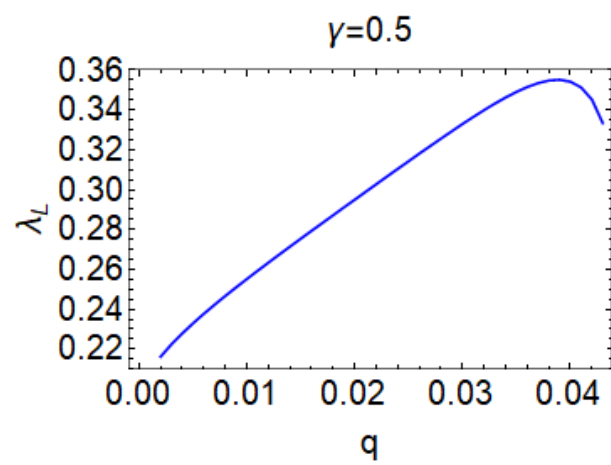
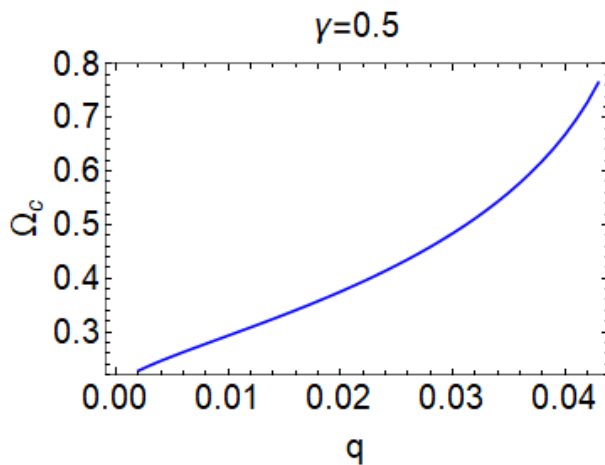
In the remaining of this section, we think that it is necessary to investigate constraints on the new family of ABG black holes in terms of the shadow data of the supermassive black hole in the center of the M87 galaxy detected by the EHT. Based on the observations [16, 64–66], the angular size of the shadow of the M87* black hole is $\delta = (42 \pm 3) \mu\text{as}$ (microarcsecond), the distance to the black hole $D = 16.8^{+0.8}_{-0.8}$ Mpc (million parsec), and the black hole mass $m = (6.5 \pm 0.7) \times 10^9 M_\odot$. As a result, the shadow diameter $d_{\text{M87*}}$ in terms of the unit of mass is [64, 65]

$$d_{\text{M87*}} \equiv \frac{D\delta}{m} \approx 11.0 \pm 1.5, \quad (19)$$

which means that the range of the shadow diameter is $9.5 \lesssim d_{\text{M87*}} = 2R_{\text{sh}} \lesssim 12.5$ in the 1σ confidence region and $8.0 \lesssim d_{\text{M87*}} = 2R_{\text{sh}} \lesssim 14.0$ in the 2σ confidence region.

We plot the allowed regions in the parameter space (γ, q) for the new family of ABG black holes in accordance with the shadow diameter $d_{\text{M87*}}$ in the 1σ and 2σ confidence regions in Figs. 10 and 11, respectively, in which we also give the range of the angular velocity Ω_c that connects the real part of the quasinormal mode frequencies $\omega_{l \gg 1}$ in the eikonal limit in the parameter space (γ, q) .

In the 1σ confidence region, we can see from Fig. 10 that the increase of γ makes the allowable range of q become large. Especially for the new family of ABG black holes with $0 < \gamma < 1$, the allowed charge q is less than 0.0809, while for this family of black holes with $1 < \gamma < \infty$, the allowed charge q is less than



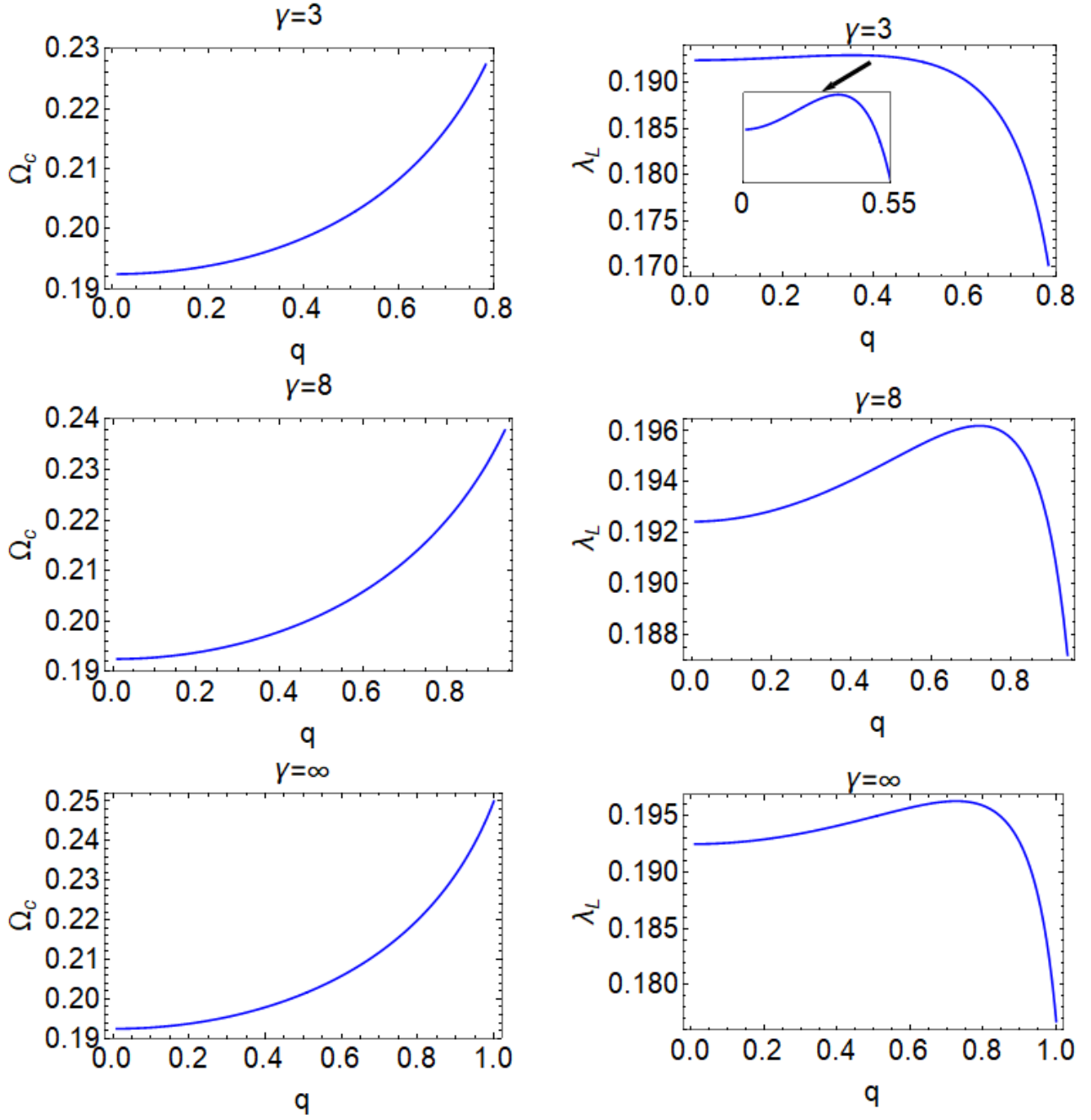


Fig. 6. The angular velocity Ω_c and the Lyapunov exponent λ_L with respect to the charge q when γ is given for different cases, where the case of $\gamma = 2$ corresponding to the ABG black hole and the case of $\gamma \rightarrow \infty$ to the Reissner-Nordström black hole are attached for comparison. Here we set $m = 1$.

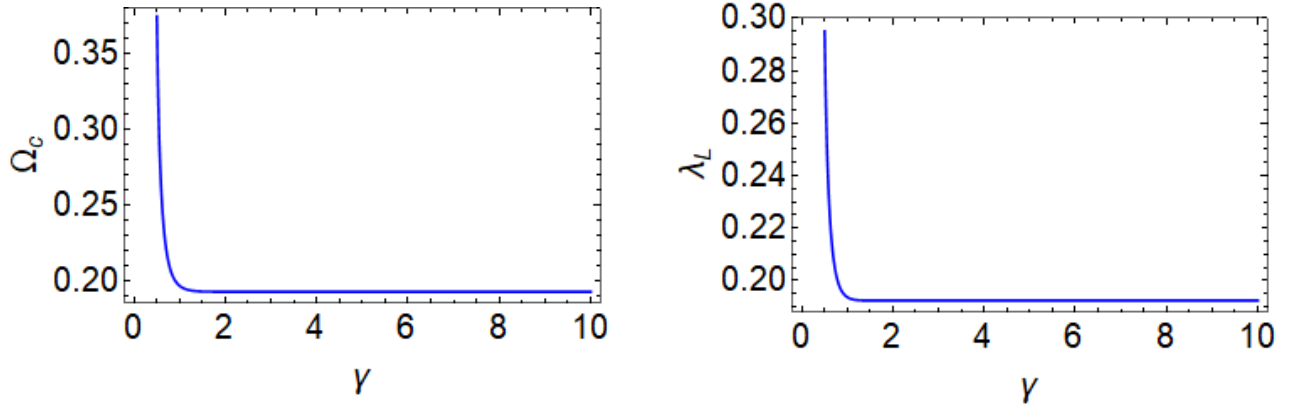


Fig. 7. The angular velocity Ω_c and the Lyapunov exponent λ_L with respect to the parameters γ . Here we set $m = 1$ and $q = 0.02$.

0.6806. In addition, we can find that the range of the allowable angular velocity Ω_c of the new black holes is $0.1925 < \Omega_c \leq 0.2105$ for all values of γ , where the equality corresponds to the case of the upper limit of the charge q under different values of γ in the left graph. The right graph implies that it is impossible to impose constraints on the parameter γ in terms of Ω_c or R_{sh} .

In the 2σ confidence region, we can see from Fig. 11 that the increase of the parameter γ makes the allowable range of the charge q become large. Especially for the new family of ABG black holes with $0 < \gamma < 1$, the allowed charge q is less than 0.1941, while for this family of black holes with $1 < \gamma < \infty$, the allowed charge q is less than 1. In addition, we can see that the range of the allowable angular velocity Ω_c is $0.1925 < \Omega_c \leq 0.25$ for the case of $0 < \gamma \leq 1.5$. For the case of $1.5 < \gamma < \infty$, the increase of γ makes the allowable range of the angular velocity decrease to the minimum range at first, $0.1925 < \Omega_c \leq 0.2275$ at $\gamma = 3$, and then increase to the maximum range, $0.1925 < \Omega_c \leq 0.25$ at $\gamma \rightarrow \infty$.

In Figs. 10 and 11 the black, red, and green points are associated with special values of γ . Now we use the sixth-order WKB approximation method to calculate the fundamental quasinormal mode frequencies of massless scalar field perturbations by taking such a range of γ that includes these special points. The results are shown in Table 1.

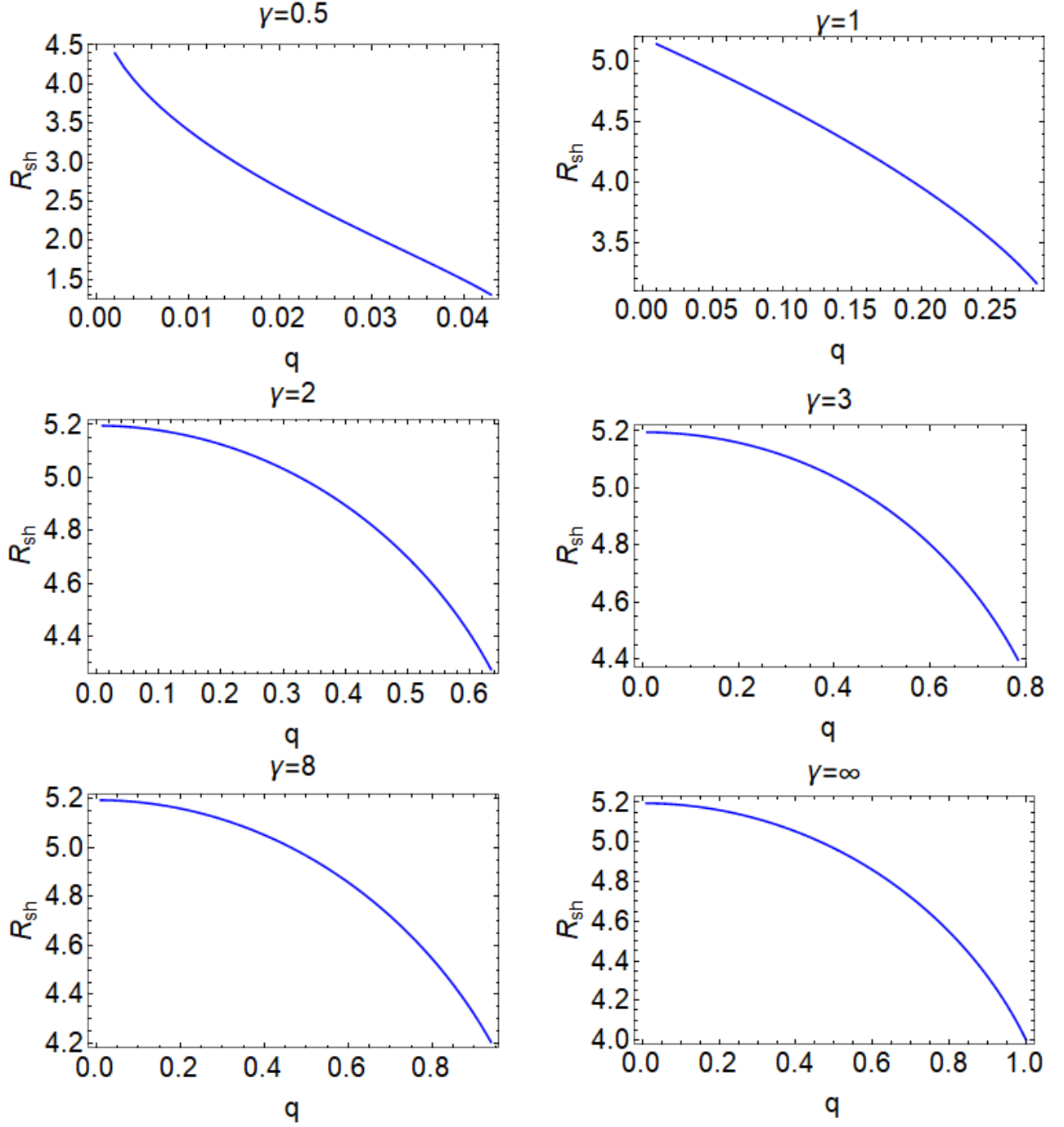


Fig. 8. The shadow radius R_{sh} with respect to the charge q when γ is given for different cases, where the case of $\gamma = 2$ corresponding to the ABG black hole and the case of $\gamma \rightarrow \infty$ to the Reissner-Nordström black hole are attached for comparison. Here we set $m = 1$.

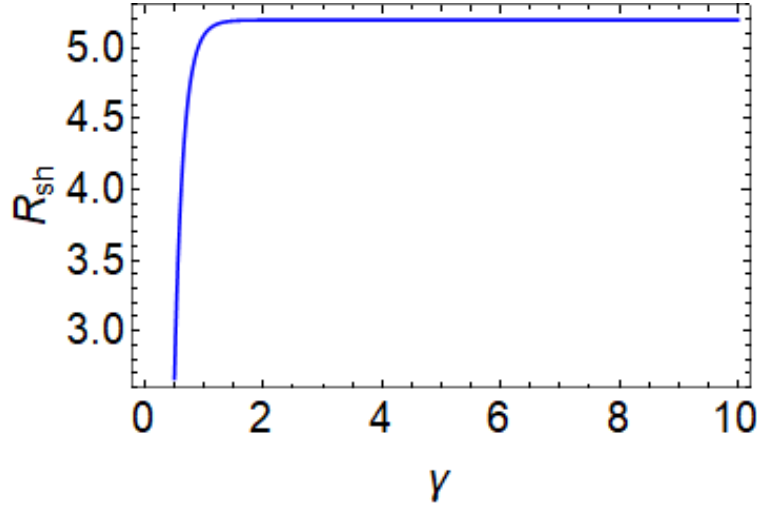


Fig. 9. The shadow radius R_{sh} with respect to the parameter γ . Here we set $m = 1$ and $q = 0.02$.

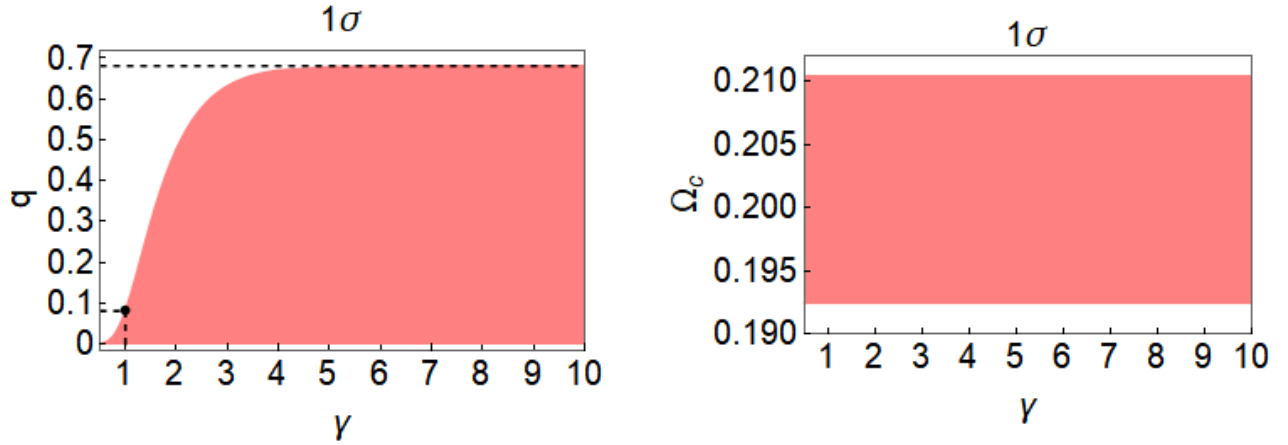


Fig. 10. The area shaded in pink on the left shows the allowed region in the parameter space (γ, q) for the new family of ABG black holes, which is plotted in accordance with the shadow diameter of the *M87** black hole detected by the EHT in the 1σ confidence region. The upper dotted line indicates the allowable maximum charge, 0.6806, for the case of $\gamma \rightarrow \infty$, and the lower one gives the corresponding value, 0.0809, for the case of $\gamma = 1$, where the black point is located at $(1, 0.0809)$. The shaded area on the right gives the range of the allowable angular velocity Ω_c , $0.1925 < \Omega_c \leq 0.2105$, for all values of γ , where the equality corresponds to the case of the upper limit of the charge q under different values of γ in the left graph. Note that the angular velocity is calculated within the parameter space (γ, q) fixed by the left graph. Here we set $m = 1$.

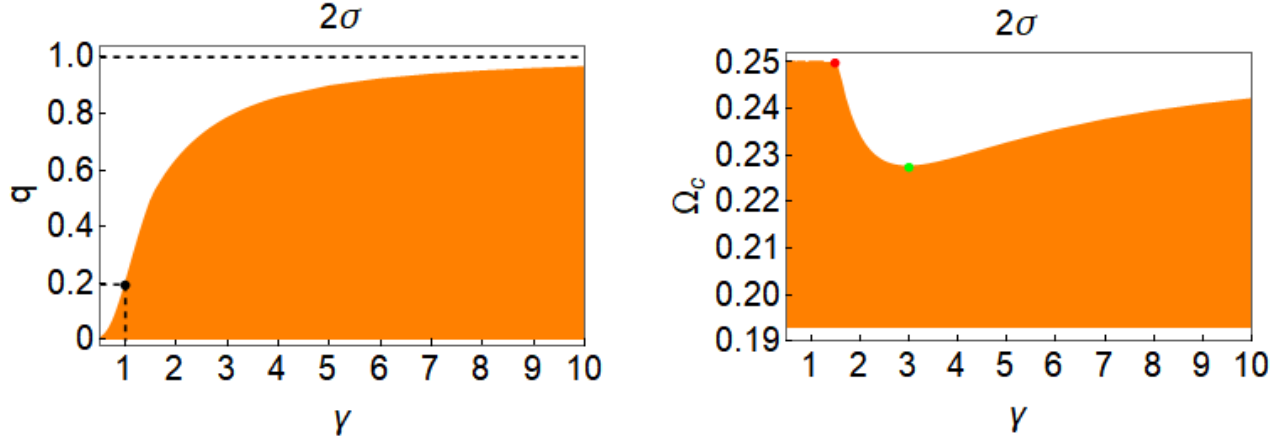


Fig. 11. The area shaded in orange on the left shows the allowed region in the parameter space (γ, q) for the new family of ABG black holes, which is plotted in accordance with the shadow diameter of the $M87^*$ black hole detected by the EHT in the 2σ confidence region. The upper dotted line indicates the allowable maximum charge, 1, for the case of $\gamma \rightarrow \infty$, and the lower one gives the corresponding value, 0.1941, for the case of $\gamma = 1$, where the black point is located at $(1, 0.1941)$. The shaded area on the right gives the range of the allowable angular velocity Ω_c , where the parameter space (γ, q) has been fixed in the left graph. The red point is located at $(1.5, 0.25)$ and the green one at $(3, 0.2275)$. The range of the allowable angular velocity is $0.1925 < \Omega_c \leq 0.25$ for the cases of $0 < \gamma \leq 1.5$ and $\gamma \rightarrow \infty$, where the equality corresponds to the case of the upper limit of the charge q under different values of γ in the left graph. Here we set $m = 1$.

Table 1: The quasinormal mode frequencies of massless scalar field perturbations for the new family of ABG black holes are computed in the allowed regions of the parameter space (γ, q) in the 1σ and 2σ confidence regions.

$m = 1, l = 1, n = 0$			
γ	1σ or 2σ	1σ	2σ
	ω_{min}	ω_{1max}	ω_{2max}
0.5	$0.29291 - 0.0977616i$	$0.320407 - 0.103985i$	$0.380271 - 0.116588i$
1		$0.320705 - 0.100095i$	$0.380517 - 0.101529i$
1.5		$0.321042 - 0.0959725i$	$0.377801 - 0.0816016i$
2		$0.321066 - 0.0940529i$	$0.353446 - 0.0814751i$
3		$0.320781 - 0.095721i$	$0.343584 - 0.0862216i$
4		$0.320749 - 0.0978395i$	$0.346517 - 0.0895958i$
5		$0.320819 - 0.0987367i$	$0.351123 - 0.0912991i$
6		$0.320836 - 0.0990882i$	$0.356101 - 0.0918408i$
7		$0.320808 - 0.0992539i$	$0.360232 - 0.0921007i$
8		$0.320776 - 0.0993385i$	$0.361658 - 0.0929356i$
∞		$0.320765 - 0.0993989i$	$0.377706 - 0.0893423i$

Moreover, by taking $m = 6.5 \times 10^9 M_\odot$ and using the formula,

$$f = \frac{\text{Re}(\omega)}{2\pi m} \times \frac{c^3}{G}, \quad (20)$$

we convert the oscillation frequencies $\text{Re}(\omega)$ in Table 1 to their values f in terms of the unit of Hertz (Hz). The results are shown in Table 2.

Table 2: The oscillation frequencies f of massless scalar field perturbations for the new family of ABG black holes are computed in the allowed regions of the parameter space (γ, q) in the 1σ and 2σ confidence regions.

$m = 6.5 \times 10^9 M_\odot, l = 1, n = 0$			
γ	$1\sigma \text{ or } 2\sigma$	1σ	2σ
	$f_{\min} (10^{-6} \text{Hz})$	$f_{1\max} (10^{-6} \text{Hz})$	$f_{2\max} (10^{-6} \text{Hz})$
0.5	1.456	1.593	1.890
1		1.594	1.891
1.5		1.596	1.878
2		1.596	1.757
3		1.594	1.708
4		1.594	1.722
5		1.595	1.745
6		1.595	1.770
7		1.595	1.791
8		1.594	1.798
∞		1.594	1.877

From the two figures and two tables we have the following conclusions:

- The frequency range of the fundamental mode with $l = 1$ matching the shadow diameter of the $M87^*$ black hole detected by EHT is about $1.4 \times 10^{-6} \text{Hz} \sim 1.9 \times 10^{-6} \text{Hz}$.
- In the 1σ confidence region, it is extremely difficult to constrain γ by using the quasinormal mode frequencies. While in the 2σ confidence region, it is possible to exclude certain range of γ in terms of the quasinormal mode frequencies. For example, if f is about $1.8 \times 10^{-6} \text{Hz} \sim 1.9 \times 10^{-6} \text{Hz}$, then $\gamma \notin [2, 8]$.

6 Conclusion

In this paper, we construct a type of ABG related black holes with five parameters and confirm its regularity if the conditions: $\alpha\gamma \geq 6$, $\beta\gamma \geq 8$, and $\gamma > 0$, are satisfied. Then we just consider the saturated case of these conditions, i.e. $\alpha = 6/\gamma$ and $\beta = 8/\gamma$, and give a new family of ABG black holes associated with only three parameters, m , q , and γ . For this new family of ABG black holes, we investigate its thermodynamic and dynamic properties, such as Hawking temperature, quasinormal mode frequency, and shadow radius. By comparing the properties with those of the ABG black hole and Reissner-Nordström black hole, we determine the characteristics of the new ABG model. Finally, we use the shadow data of the $M87^*$ black hole detected by the EHT to give some constraints on the new family of ABG black holes. Here we summarize the major ones.

- The behaviour of the Hawking temperature with respect to the horizon radius is similar to that of the ABG black hole and Reissner-Nordström black hole. For a fixed q , the maximum Hawking

temperature depends on the parameter γ , more precisely, it is less than that of the ABG black hole when γ is less than 2, and larger than that of the ABG black hole when γ is larger than 2. In any case, the maximum Hawking temperature is less than that of the Reissner-Nordström black hole, but their difference becomes small when γ is large.

- The behaviour of the real parts of quasinormal modes with respect to charge q is similar to that of the ABG black hole and Reissner-Nordström black hole. This shows that the oscillation law of the new ABG black hole is similar to that of the ABG black hole and Reissner-Nordström black hole.
- The behaviour of the negative imaginary parts of quasinormal modes with respect to charge q is completely different from that of the ABG black hole but similar to that of the Reissner-Nordström black hole. This means that the decay law of the new ABG black hole is completely different from that of the ABG black hole but similar to that of the Reissner-Nordström black hole.
- The behaviour of the shadow radii with respect to charge q is similar to that of the ABG black hole and Reissner-Nordström black hole. This is obvious because the shadow radius is just the reciprocal of the real parts of quasinormal modes under certain conditions [51, 52, 62, 63].
- The shadow data of the $M87^*$ black hole detected by the EHT impose an upper limit on the charge q of the new family of ABG black holes. This upper limit increases rapidly at first and then slowly but does not exceed the mass of the $M87^*$ black hole at last when the parameter γ is increasing and going to infinity. In addition, the data restrict the frequency range of the fundamental mode with $l = 1$ to $1.4 \times 10^{-6} Hz \sim 1.9 \times 10^{-6} Hz$.

Acknowledgments

This work was supported in part by the National Natural Science Foundation of China under Grant No. 11675081. The authors would like to thank the anonymous referee for the helpful comments that improve this work greatly.

References

- [1] R. Penrose, *Gravitational collapse and space-time singularities*, Phys. Rev. Lett. **14** (1965) 57.
- [2] S.W. Hawking, *Occurrence of singularities in open universes*, Phys. Rev. Lett. **15** (1965) 689.
- [3] R. Penrose, *Gravitational collapse: The role of general relativity*, Riv. Nuovo Cimento **1** (1969) 252.
- [4] S.W. Hawking and G. F. R. Ellis, *The Large Scale Structure of Space-Time*, Cambridge University Press, Cambridge, England, 1973.
- [5] Z-Y. Fan and X. Wang, *Construction of regular black holes in general relativity*, Phys. Rev. **D 94** (2016) 124027 [arXiv:1610.02636 [gr-qc]].

- [6] J.M. Bardeen, *Non-singular general relativistic gravitational collapse*, in Proceedings of the International Conference GR5, Tbilisi, Georgia, 1968, p. 174.
- [7] E. Ayón-Beato and A. García, *Regular black hole in general relativity coupled to nonlinear electrodynamics*, Phys. Rev. Lett. **80** (1998) 5056.
- [8] E. Ayón-Beato and A. García, *New regular black hole solution from nonlinear electrodynamics*, Phys. Lett. **B 464** (1999) 25 [arXiv:hep-th/9911174].
- [9] E. Ayón-Beato and A. García, *The Bardeen model as a nonlinear magnetic monopole*, Phys. Lett. **B 493** (2000) 149 [arXiv:gr-qc/0009077].
- [10] E. Ayón-Beato and A. García, *Four-parametric regular black hole solution*, Gen. Relativ. Gravit. **37** (2005) 635 [arXiv:gr-qc/0403229].
- [11] L. Balart and E.C. Vagenas, *Regular black holes with a nonlinear electrodynamics source*, Phys. Rev. **D 90** (2014) 124045 [arXiv:1408.0306 [gr-qc]].
- [12] M.-S. Ma, *Magnetically charged regular black hole in a model of nonlinear electrodynamics*, Ann. Phys. **362** (2015) 529 [arXiv:1509.05580 [gr-qc]].
- [13] E.L. Junior, M.E. Rodrigues, and M.J. Houndjo, *Regular black holes in $f(T)$ Gravity through a nonlinear electrodynamics source*, J. Cosmol. Astropart. Phys. **10** (2015) 060 [arXiv:1503.07857 [gr-qc]].
- [14] B.P. Abbott, *et al.*, *Directly comparing GW150914 with numerical solutions of Einstein's equations for binary black hole coalescence*, Phys. Rev. **D 94** (2016) 064035 [arXiv:1606.01262 [gr-qc]].
- [15] B.P. Abbott, *et al.*, *GW170817: Observation of gravitational waves from a binary neutron star inspiral*, Phys. Rev. Lett **119** (2017) 161101 [arXiv:1710.05832 [gr-qc]].
- [16] EHT Collaboration, *First M87 event horizon telescope results. I. The shadow of the supermassive black hole*, Astrophys. J. **875** (2019) L1 [arXiv:1906.11238 [astro-ph.GA]].
- [17] EHT Collaboration, *First M87 event horizon telescope results. IV. Imaging the central supermassive black hole*, Astrophys. J. **875** (2019) L4 [arXiv:1906.11241 [astro-ph.GA]].
- [18] K.D. Kokkotas and B.G. Schmidt, *Quasinormal modes of stars and black holes*, Living Rev. Relativity **2** (1999) 2 [arXiv:gr-qc/9909058].
- [19] H.P. Nollert, *Quasinormal modes: The characteristic sound of black holes and neutron stars*, Classical Quantum Gravity **16** (1999) R159.
- [20] E. Berti, V. Cardoso, and A.O. Starinets, *Quasinormal modes of black holes and black branes*, Classical Quantum Gravity **26** (2009) 163001 [arXiv:0905.2975 [gr-qc]].
- [21] R.A. Konoplya and A. Zhidenko, *Quasinormal modes of black holes: From astrophysics to string theory*, Rev. Mod. Phys. **83** (2011) 793 [arXiv:1102.4014 [gr-qc]].

- [22] R.A. Konoplya, *Decay of a charged scalar field around a black hole: Quasinormal modes of RN, RNAdS, and dilaton black holes*, Phys. Rev. **D 66** (2002) 084007 [arXiv:gr-qc/0207028].
- [23] R.A. Konoplya, *Massive charged scalar field in a Reissner–Nordstrom black hole background: quasinormal ringing*, Phys. Lett. **B 550** (2002) 117 [arXiv:gr-qc/0210105].
- [24] R.A. Konoplya, *Gravitational quasinormal radiation of higher-dimensional black holes*, Phys. Rev. **D 68** (2003) 124017 [arXiv:hep-th/0309030].
- [25] R.A. Konoplya, *Quasinormal modes of the charged black hole in Gauss-Bonnet gravity*, Phys. Rev. **D 71** (2005) 024038 [arXiv:hep-th/0410057].
- [26] A. Flachi and J. Lemos, *Quasinormal modes of regular black holes*, Phys. Rev. **D 87** (2013) 024034 [arXiv:1211.6212 [gr-qc]].
- [27] B. Toshmatov, A. Abdujabbarov, Z. Stuchlík, and B. Ahmedov, *Quasinormal modes of test fields around regular black holes*, Phys. Rev. **D 91** (2015) 083008 [arXiv:1503.05737 [gr-qc]].
- [28] G. Panotopoulos and A. Rincon, *Quasinormal modes of regular black holes with non-linear electrodynamical sources*, Eur. Phys. J. Plus **134** (2019) 300 [arXiv:1904.10847 [gr-qc]].
- [29] J. Li, H. Ma, and K. Lin, *Dirac quasinormal modes in spherically symmetric regular black holes*, Phys. Rev. **D 88** (2013) 064001 [arXiv:1308.6499 [gr-qc]].
- [30] K. Jusufi, *et al.*, *Quasinormal modes, quasiperiodic oscillations, and the shadow of rotating regular black holes in nonminimally coupled Einstein-Yang-Mills theory*, Phys. Rev. **D 103** (2021) 024013 [arXiv:2008.08450 [gr-qc]].
- [31] K. Jusufi, M. Amir, M.S. Ali, and S.D. Maharaj, *Quasinormal modes, shadow, and greybody factors of 5D electrically charged Bardeen black holes*, Phys. Rev. **D 102** (2020) 064020 [arXiv:2005.11080 [gr-qc]].
- [32] S. Fernando and J. Correa, *Quasinormal modes of the Bardeen black hole: Scalar perturbations*, Phys. Rev. **D 86** (2012) 064039 [arXiv:1208.5442 [gr-qc]].
- [33] C. Wu, *Quasinormal frequencies of gravitational perturbation in regular black hole spacetimes*, Eur. Phys. J. **C 78** (2018) 283.
- [34] B. Toshmatov, Z. Stuchlík, J. Schee, and B. Ahmedov, *Electromagnetic perturbations of black holes in general relativity coupled to nonlinear electrodynamics*, Phys. Rev. **D 97** (2018) 084058 [arXiv:1805.00240 [gr-qc]].
- [35] B. Toshmatov, Z. Stuchlík, and B. Ahmedov, *Electromagnetic perturbations of black holes in general relativity coupled to nonlinear electrodynamics: Polar perturbations*, Phys. Rev. **D 98** (2018) 085021 [arXiv:1810.06383 [gr-qc]].

- [36] B. Toshmatov, Z. Stuchlík, B. Ahmedov, and D. Malafarina, *Relaxations of perturbations of space-times in general relativity coupled to nonlinear electrodynamics*, Phys. Rev. **D 99** (2019) 064043 [arXiv:1903.03778 [gr-qc]].
- [37] J.L. Synge, *The escape of photons from gravitationally intense stars*, Mon. Not. Roy. Astron. Soc. **131** (1966) 463.
- [38] J.-P. Luminet, *Image of a spherical black hole with thin accretion disk*, Astron. Astrophys. **75** (1979) 228.
- [39] A. De Vries, *The apparent shape of a rotating charged black hole, closed photon orbits and the bifurcation set A4*, Class. Quantum Grav. **17** (2000) 123.
- [40] K. Hioki and U. Miyamoto, *Hidden symmetries, null geodesics, and photon capture in the Sen black hole*, Phys. Rev. **D 78** (2008) 044007 [arXiv:0805.3146 [gr-qc]].
- [41] C. Bambi and K. Freese, *Apparent shape of super-spinning black holes*, Phys. Rev. **D 79** (2009) 043002 [arXiv:0812.1328 [astro-ph]].
- [42] A. Grenzebach, V. Perlick, and C. Lämmerzahl, *Photon regions and shadows of Kerr-Newman-NUT black holes with a cosmological constant*, Phys. Rev. **D 89** (2014) 124004 [arXiv:1403.5234 [gr-qc]].
- [43] M. Guo, N.A. Obers, and H. Yan, *Observational signatures of near-extremal Kerr-like black holes in a modified gravity theory at the Event Horizon Telescope*, Phys. Rev. **D 98** (2018) 084063 [arXiv:1806.05249 [gr-qc]].
- [44] R.A. Hennigar, M.B.J. Poshteh, and R.B. Mann, *Shadows, signals, and stability in Einsteinian cubic gravity*, Phys. Rev. **D 97** (2018) 064041 [arXiv:1801.03223 [gr-qc]].
- [45] G.S. Bisnovatyi-Kogan and O.Y. Tsupko, *Shadow of a black hole at cosmological distances*, Phys. Rev. **D 98** (2018) 084020 [arXiv:1805.03311 [gr-qc]].
- [46] V. Perlick, O.Y. Tsupko, and G.S. Bisnovatyi-Kogan, *Black hole shadow in an expanding universe with a cosmological constant*, Phys. Rev. **D 97** (2018) 104062 [arXiv:1804.04898 [gr-qc]].
- [47] A. Abdujabbarov, M. Amir, B. Ahmedov, and S.G. Ghosh, *Shadow of rotating regular black holes*, Phys. Rev. **D 93** (2016) 104004 [arXiv:1604.03809 [gr-qc]].
- [48] R. Kumar, S.G. Ghosh, and A.-Z. Wang, *Shadow cast and deflection of light by charged rotating regular black holes*, Phys. Rev. **D 100** (2019) 124024 [arXiv:1912.05154 [gr-qc]].
- [49] N. Tsukamoto, *Black hole shadow in an asymptotically flat, stationary, and axisymmetric space-time: The Kerr-Newman and rotating regular black holes*, Phys. Rev. **D 97** (2018) 064021 [arXiv:1708.07427 [gr-qc]].

- [50] R.A. Konoplya and A. Zhidenko, *Analytical representation for metrics of scalarized Einstein-Maxwell black holes and their shadows*, Phys. Rev. **D 100** (2019) 044015 [arXiv:1907.05551 [gr-qc]].
- [51] H. Lu and H.-D. Lyu, *Schwarzschild black holes have the largest size*, Phys. Rev. **D 101** (2020) 044059 [arXiv:1911.02019 [gr-qc]].
- [52] M. Zhang and M. Guo, *Can shadows reflect phase structures of black holes?*, Eur. Phys. J. **C 80** (2020) 1 [arXiv:1909.07033 [gr-qc]].
- [53] J.M. Bardeen, B. Carter, and S.W. Hawking, *The four laws of black hole mechanics*, Commun. Math. Phys. **31** (1973) 161.
- [54] S.W. Hawking, *Particle creation by black holes*, Commun. Math. Phys. **43** (1975) 199.
- [55] B.F. Schutz and C.M. Will, *Black hole normal modes: A semianalytic approach*, Astrophys. Jour. Lett. **291** (1985) L33.
- [56] S. Iyer and C.M. Will, *Black-hole normal modes: A WKB approach. I. Foundations and application of a higher-order WKB analysis of potential-barrier scattering*, Phys. Rev. **D 35** (1987) 3621.
- [57] R.A. Konoplya, *Quasinormal behavior of the D-dimensional Schwarzschild black hole and the higher order WKB approach*, Phys. Rev. **D 68** (2003) 024018 [arXiv:hep-th/0303052].
- [58] J. Matyjasek and M. Opala, *Quasinormal modes of black holes: The improved semianalytic approach*, Phys. Rev. **D 96** (2017) 024011 [arXiv:1704.00361 [gr-qc]].
- [59] V. Cardoso, A.S. Miranda, E. Berti, H. Witek, and V.T. Zanchin, *Geodesic stability, Lyapunov exponents, and quasinormal modes*, Phys. Rev. **D 79** (2009) 064016 [arXiv:0812.1806 [hep-th]].
- [60] R.A. Konoplya and A. Zhidenko, *The portrait of eikonal instability in Lovelock theories*, J. Cosmol. Astropart. Phys. **05** (2017) 050 [arXiv:1705.01656 [gr-qc]].
- [61] R.A. Konoplya and Z. Stuchlík, *Are eikonal quasinormal modes linked to the unstable circular null geodesics?*, Phys. Lett. **B 771** (2017) 597 [arXiv:1705.05928 [gr-qc]].
- [62] K. Jusufi, *Quasinormal modes of black holes surrounded by dark matter and their connection with the shadow radius*, Phys. Rev. **D 101** (2020) 084055 [arXiv:1912.13320 [gr-qc]].
- [63] B. Cuadros-Melgar, R.D.B. Fontana, and J. de Oliveira, *Analytical correspondence between shadow radius and black hole quasinormal frequencies*, Phys. Lett. **B 811** (2020) 135966 [arXiv:2005.09761 [gr-qc]].
- [64] C. Bambi, K. Freese, S. Vagnozzi, and L. Visinelli, *Testing the rotational nature of the supermassive object M87* from the circularity and size of its first image*, Phys. Rev. **D 100** (2019) 044057 [arXiv:1904.12983 [gr-qc]].

- [65] A. Allahyari, M. Khodadi, S. Vagnozzi, and D.F. Mota, *Magnetically charged black holes from non-linear electrodynamics and the Event Horizon Telescope*, J. Cosmol. Astropart. Phys. **02** (2020) 003 [arXiv:1912.08231 [gr-qc]].
- [66] R. Kumar, A. Kumar, and S.G. Ghosh, *Testing Rotating Regular Metrics as Candidates for Astrophysical Black Holes*, Astrophys. J. **896** (2020) 89 [arXiv:2006.09869 [gr-qc]].